Available online at www.sciencedirect.com
SCIENCE DIRECT®
Catalysis Today 105 (2005) 367–371
CATALYSIS TODAY
www.elsevier.com/locate/cattod

Partial oxidation of methane to synthesis gas over corundum supported mixed oxides: One channel studies

S. Pavlova *, N. Sazonova, V. Sadykov, S. Pokrovskaya, V. Kuzmin, G. Alikina, A. Lukashevich, E. Gubanova

Boreskov Institute of Catalysis, Novosibirsk State University, Siberian Branch of the Russian Academy of Sciences, pr. Lavrentieva 5, 630090 Novosibirsk, Russia

Available online 11 July 2005

Abstract

Catalytic partial oxidation of methane (POM) over the monolithic catalyst $LaNiO_x/CeO_2–ZrO_2/\alpha\text{-}Al_2O_3$ has been studied. Experiments were conducted with one channel of a monolith at a varied channel length, contact time (~1–6 ms) and temperature using the diluted gas mixture (1% CH_4 + 0.5% O_2 in He). At increasing temperature and contact time, CO selectivity rises within the whole temperature range whereas the contact time dependence of H_2/CO ratio varies with the temperature. These results support the POM reaction scheme including primary formation of CO and H_2 followed by their oxidation in the presence of gas-phase O_2. Steam and dry methane reforming reactions occur in the part of monolithic channel where oxygen is absent, thus increasing syngas yield.

Keywords: Partial oxidation of methane; Syngas; Channel of monolith; $LaNiO_x/CeO_2–ZrO_2/\alpha\text{-}Al_2O_3$

1. Introduction

Catalytic partial oxidation of methane at short contact times is now considered as an attractive technology for the small-scale and distributed production of syngas in the stationary and mobile fuel processing [1]. POM can also be integrated into stage combustors of methane for gas turbines wherein methane is partially oxidized in the fuel-rich combustor followed by the fuel-lean combustion [2]. In view of such applications, realization of the process at contact times <0.1 s to miniaturize the reactors is the most promising route, which determines the use of monolithic catalysts having a high surface to volume ratio and a low pressure drop [3–4]. Previous studies of POM using monolithic catalysts and structured reactors (e.g. annular or flat-plate reactors) have been carried out mainly over catalysts containing Pt or Rh [5–9]. Noble metals have a high cost and limited availability whereas inexpensive Ni-containing catalysts possessing the high activity for POM are preferred from industrial standpoint [10]. However, though POM extensively has been studied on granulated catalysts [1,10], the structured Ni catalysts were used only in a few works (see, e.g. [11]). The catalysts comprised of $LaNiO_x$ and $CeO_2–ZrO_2$ supported on $\alpha\text{-}Al_2O_3$ pellets were shown earlier [12] to be active and stable catalysts in this process. A high oxygen mobility in fluorite-like $CeO_2–ZrO_2$ solid solutions helps to ensure an efficient performance of perovskite-type $LaNiO_3$ in POM.

In this work, POM was studied over the catalysts containing $LaNiO_3$ and $CeO_2–ZrO_2$ solid solution supported on the corundum monolith. To investigate the reaction kinetics and to elucidate the mass transfer effects, experiments were conducted with one channel of a monolithic catalyst at a varied channel length, space velocity and temperature. Extremely short contact times ~1–6 ms allow to analyze the process far from the thermodynamic equilibrium constraints. To prevent hot-spots, temperature gradients and homogeneous gas-phase reactions, diluted gas mixtures were used. The nature of the

* Corresponding author. Tel.: +7 383 3307 672; fax: +7 383 3308 766.
E-mail address: pavlova@catalysis.nsk.su (S. Pavlova).

0920-5861/$ – see front matter © 2005 Elsevier B.V. All rights reserved.
doi:10.1016/j.cattod.2005.06.030

POM routes (direct formation of CO and H_2 or indirect one involving combustion of CH_4 to CO_2 and H_2O followed by reforming reactions of remaining methane) is discussed.

2. Experimental

As supports, separate triangular channels of α-Al_2O_3 monolith (specific surface area of 3 m^2/g) annealed at 1300 °C with the wall thickness 0.2 mm, the side of the inside triangle 2.33 mm and the length of 4–30 mm were used. The $Zr_{0.8}Ce_{0.2}O_2$ and $LaNiO_x$ were successively supported by the incipient wetness impregnation first with the mixed solution of $Ce(NO_3)_3$ and $ZrOCl_2$, and then with the solution of La and Ni nitrates as described in [12]. After each impregnation, samples were dried and calcined at 900 °C in air. The $Zr_{0.8}Ce_{0.2}O_2$ content in the catalysts was 10 wt.%, and $LaNiO_x$ content was 7 wt.%. According to the previous study [12], the $LaNiO_3$ perovskite phase of the hexagonal structure and $Zr_{0.8}Ce_{0.2}O_2$ solid solution are present in the catalysts.

The POM testing of the catalysts was carried out in a plug-flow quartz reactor of 4 mm inner diameter. The space between the catalyst channel and the reactor walls was sealed up with α-Al_2O_3 fiber. The temperature of the catalytic bed varied in the range of 600–900 °C was measured by a thermocouple situated outside the reactor. The catalysts were pretreated in situ at 900 °C for 1 h in the oxygen flow. Then, at the same temperature, the reaction mixture (1 vol.% CH_4, 0.5% O_2, He—balance) was fed with the flow rate in the range of 70–300 cm^3/min, i.e. at 0.7–6 ms contact time estimated by using only the channel walls volume. Isothermal conditions were kept due to a highly diluted feed. Blank experiments verified that homogeneous reactions did not occur under studied conditions. The reagents and reaction products were analyzed by GC as in [12].

Temperature-programmed POM reaction for channels subjected to different pretreatments in 2 vol.% O_2 in He, 2 vol.% H_2 in He, 1 vol.% CH_4 in He were studied using the same feed following earlier described procedures [13].

3. Results and discussion

3.1. Effect of the temperature

The temperature dependence of methane and oxygen conversions along with CO selectivity for channels of different length (at the 300 ml/min feed rate) are shown in Figs. 1–3. The conversion of reactants and CO selectivity increase with the temperature and the channel length. For all channels, within the whole studied temperature range, the conversion of methane is significantly lower than the equilibrium value (Fig. 1).

Calculated equilibrium oxygen conversions at 600–900 °C are equal to 100%. The experimental oxygen

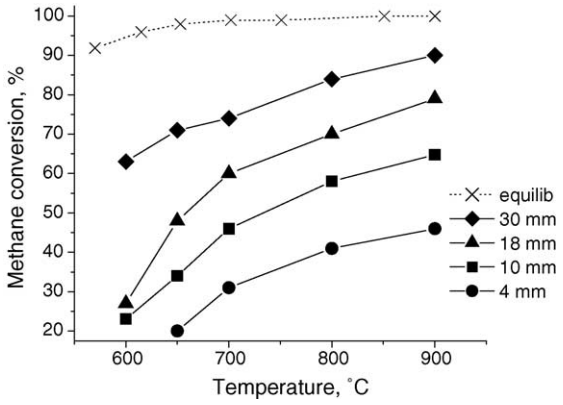

Fig. 1. Temperature dependence of equilibrium methane conversion and experimental ones over channels of 4, 10, 18 and 30 mm length, the flow rate—300 ml/min. Contact time 0.76, 1.9, 3.4 and 5.9 ms, correspondingly.

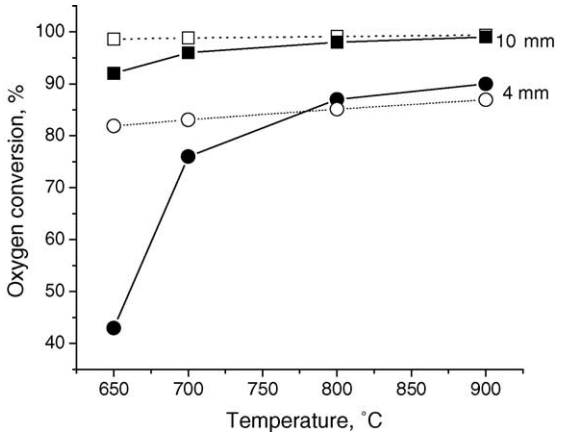

Fig. 2. Temperature dependence of oxygen conversion (calculated—dotted lines, experimental—solid lines) over 4 and 10 mm length. The flow rate—300 ml/min.

conversion is incomplete only at 650–700 °C over short channels (4 and 10 mm length) (Fig. 2). In all other cases, it is almost complete (>98%). To define conditions wherein the reaction rate could be limited by the inter-phase mass

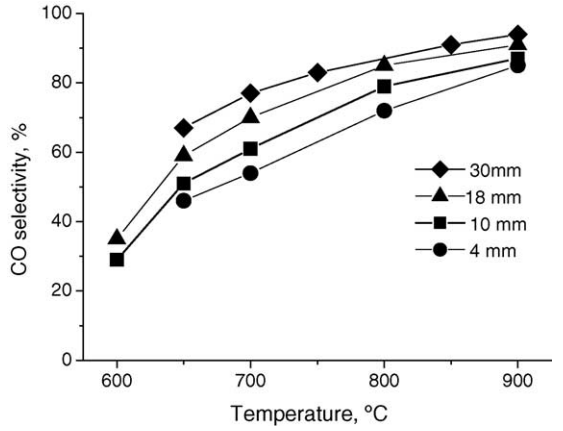

Fig. 3. Temperature dependence of CO selectivity over channels of a different length. The flow rate—300 ml/min.

transfer, the measured values of the oxygen conversion were compared with those estimated for the external diffusion controlled regime, assuming for modeling that the intrinsic rate of O_2 consumption is much higher than the mass transfer rate. The common mathematical model for the isothermal plug-flow reactor was used for these estimations [4,14]. The results are presented in Fig. 2.

The measured oxygen conversion is significantly below the calculated value only at 650 °C and contact time ~0.76 ms (for the shortest 4 mm channel). At increasing temperature and channel length, it approaches the calculated conversion. Hence, for the oxygen consumption in the catalyst channel, a regime close to the chemically controlled one could be assumed at temperatures below 650 °C and contact times ~1 ms. Mixed or pure diffusion-controlled regimes could be realized for higher temperatures and longer contact times.

3.2. Effect of the contact time

To study the effect of the contact time, the flow rate and the channel length were varied. The dependence of methane conversion on the contact time at the flow rate variation is presented in Fig. 4 for channels of different length at temperatures 700 and 900 °C. At any channel length, as the contact time increases, the methane conversion rises. Similar dependence of methane conversion is observed at increasing the channel length and keeping a constant flow rate 300 ml/min (Fig. 1). However, as the flow rate varies, the methane conversion at the same contact time differs for 10 and 18 mm channels (Fig. 4). Thus, at the contact time ~3.2 ms and 700 °C methane conversion decreases from 72 to 60% with lengthening of the channel from 10 to 18 mm and proportional increase of the flow rate from 170 to 300 cm^3/min (Fig. 4A). For these channels, at 6 ms contact time similar effect is observed at temperatures up to 900 °C (Fig. 4B). In contrary, in the case of 4 and 10 mm channels, at the same contact time the methane conversions are close irrespective of the channel length and the flow rate.

As was shown by simulation (vide supra), at temperatures exceeding 650 °C, the oxygen consumption proceeds in diffusion or mixed chemical-diffusion-controlled regimes. At the same contact time, the gas flow rate has to be higher for longer channels, which suggests a higher mass transfer rate from the gas to the channel wall. On the other hand, the Sherwood number declines rather sharply along the channel [4,11], thus decreasing the mass transfer rate. In total, this results in the decrease of the mass transfer rate for longer channels, which ensures consumption of all oxygen in a narrower inlet part of shorter channels. For such channels, the peak content of combustion products, CO_2 and H_2O, are thus expected to be higher than for longer ones. Due to respective acceleration of methane steam and dry reforming, the overall methane conversion is expected to rise.

However, further channel shortening to 4 mm does not affect the methane conversion (Fig. 4A and B) that can be caused by the axial diffusion effect. Namely, estimation of Peclet number revealed that for 4 mm channel the axial diffusion effect could be higher as well [4]. As the result, gradients of methane and oxygen concentrations along the channel decline which results in more oxidized catalyst surface, and, hence, in hampering reactions of methane steam and dry reforming. This counteracts a positive effect of external diffusion thus making methane conversion nearly constant for short channels at the same contact time.

3.3. POM scheme

For Ni-based catalysts, both direct and indirect routes of POM have been suggested [15–16]. The data obtained in the present study revealed the importance of the secondary reforming reactions favoring occurrence of the indirect pathway on Ni-containing catalysts. Indeed, methane conversion and CO selectivity increase with the temperature and the channel length (Figs. 1 and 3). At complete oxygen consumption, this is due to methane dry and steam reforming. The typical product distribution over 10 mm channel presented in Fig. 5 also agrees with occurrence of these reactions. At increasing temperature, the concentration

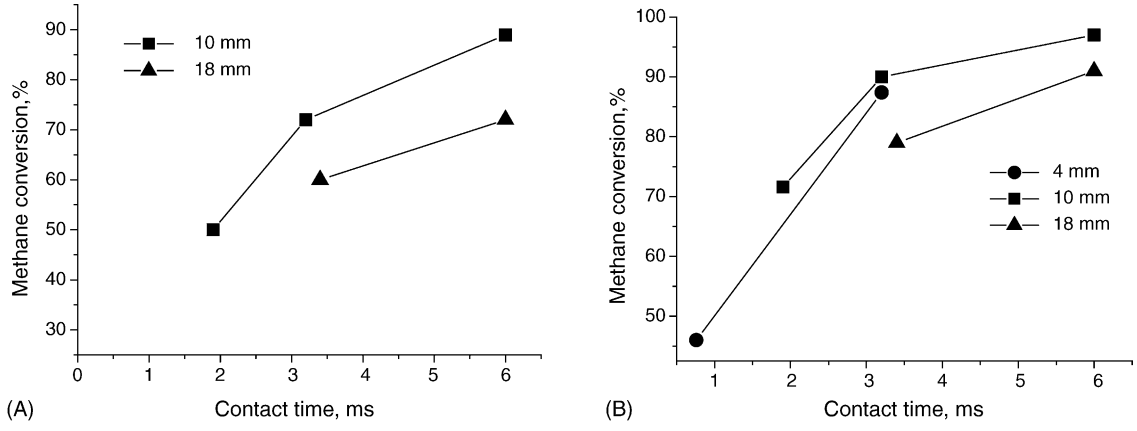

Fig. 4. Effect of the contact time on the methane conversion at 700 °C (A) and 900 °C (B). Channels of 4, 10 and 18 mm.

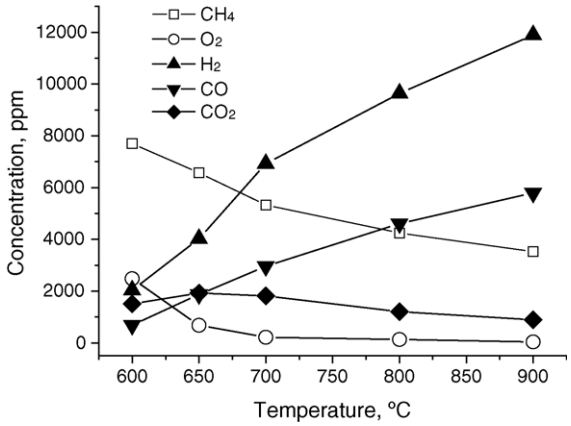

Fig. 5. Temperature dependence of methane, oxygen and product concentrations. The 10 mm channel, the flow rate—300 ml/min.

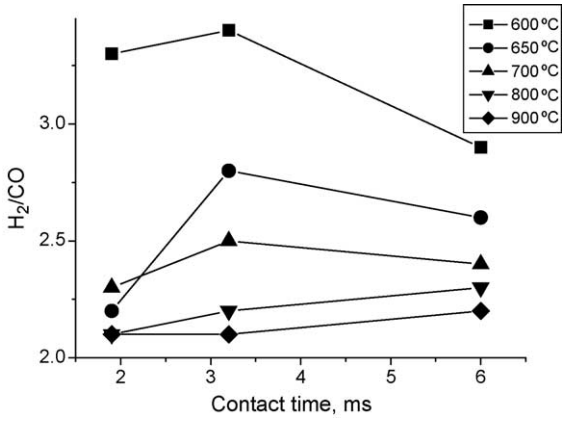

Fig. 7. Dependence of H_2/CO ratio on contact time and temperature; 10 mm channel.

of CO_2 (product of methane deep oxidation) passes through the maximum at 650 °C whereas the concentration of CO and H_2 increases so they become main products above 700 °C.

For 10 mm channel, the selectivity of CO decreases with decreasing the contact time within the whole temperature range (Fig. 6) whereas the contact time dependence of H_2/CO ratio varies with the temperature (Fig. 7). Thus, at 600–700 °C, as the CO selectivity increases with the contact time, H_2/CO ratio goes through the maximum. One can assume that the high values of H_2/CO ratio >3 observed at 600 °C and contact times <3.2 ms could be due to H_2 production via methane steam reforming and water gas shift reaction, while dry reforming is too slow in the presence of oxygen in the gas phase when Ni is oxidized. However, at these conditions, the rate of steam reforming is expected to be rather low as well. Moreover, the estimation revealed that at 600 °C the water gas shift reaction is not at equilibrium, thus suggesting its hampering by the gas phase oxygen too. This implies that the primary route of methane transformation on the Ni-containing active component includes CH_4 pyrolysis on partially oxidized Ni clusters yielding H_2 and adsorbed carbon. While hydrogen is easily desorbed into the gas phase, carbon strongly retained at the surface is oxidized into CO and, preferably, into CO_2, which explains a high H_2/CO ratio. In diffusion-controlled regime of oxygen consumption at high temperatures, decrease of the oxygen concentration at the surface favors reforming and WGS reactions while hampering CO and H_2 oxidation. Suggested scheme agrees with the results obtained by Liu et al. [16] for Ni/θ-Al_2O_3 system, where methane was suggested to be partially oxidized to CO and H_2 by the lattice oxygen of NiO.

The data of the POM temperature-programmed reaction carried out at 3.2 ms contact time over oxidized and reduced 10 mm catalyst channel are presented in Figs. 8 and 9. The dynamics of CH_4 and O_2 consumption and product evolution strongly depends upon the catalyst pretreatment suggesting its impact on the reaction route and surface reactivity. Thus, for the catalyst pre-reduced in CH_4, the first CO_2 evolution at ∼450 °C is observed due to oxidation of carbon formed on the catalyst surface during pre-reduction. Subsequent H_2O appearance at ∼530 °C implies oxidation of hydrogen

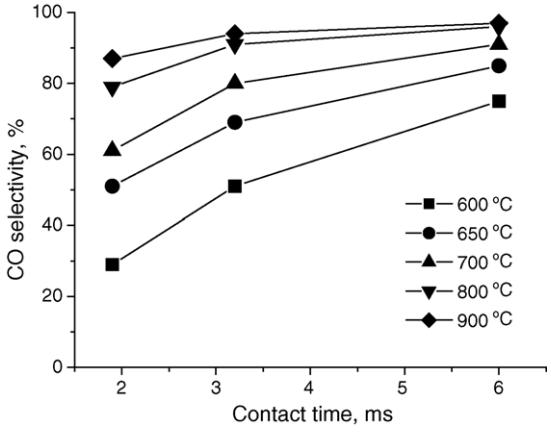

Fig. 6. Dependence of CO selectivity on the contact time and temperature; 10 mm channel.

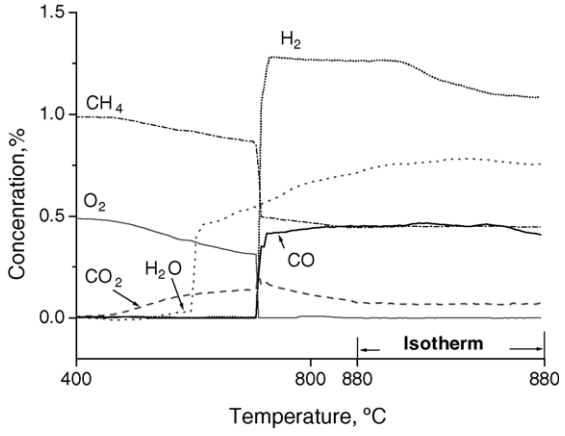

Fig. 8. Data of temperature-programmed reaction over 10 mm channel at contact time—3.2 ms. 1% CH_4 + 0.5% O_2, He—balance. The catalyst pretreated in the feed of 1% CH_4 in He.

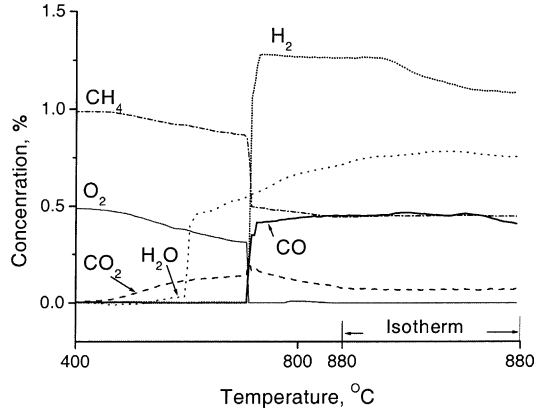

Fig. 9. Data of temperature-programmed reaction over 10 mm channel at contact time—3.2 ms. 1% CH_4 + 0.5% O_2, He—balance. The catalyst pretreated in the feed of 2% O_2 in He.

formed as a result of CH_4 pyrolysis. For oxidized catalyst, H_2O evolution at ∼550 °C followed by CO_2 appearance at ∼650 °C in the presence of oxygen in the gas phase (Fig. 9) means that pyrolysis of CH_4 can proceed over partially oxidized Ni clusters that agrees with above conclusion.

For the shortest 4 mm channel at contact time 0.76 ms, over the whole temperature range, incomplete oxygen consumption is observed, thus oxygen is present along the entire channel length. However, H_2 and CO were revealed in products even in this case. This agrees with conclusion about operation of the direct route of CO and H_2 formation followed by their subsequent combustion when gas-phase O_2 is still present.

4. Conclusion

For the reaction of POM over the monolithic catalyst comprised of corundum supported ceria–zirconia solid solution and lanthanum nickelate has been studied. One-channel experiments of such a catalyst allowed to elucidate the mass transfer effects. For oxygen consumption, a regime close to chemically controlled one is realized at temperatures below 650 °C and contact times ∼1 ms. Mixed or pure diffusion-controlled regimes can be assumed for higher temperatures and longer contact times. At increasing the temperature and contact time, CO selectivity increases within the whole temperature range whereas the contact time dependence of H_2/CO ratio varies with the temperature. These results support the POM reaction scheme including primary formation of CO and H_2 followed by their oxidation in the presence of gas-phase O_2. Steam and dry methane reforming reactions occur in the part of the monolithic channel where oxygen is absent, thus increasing syngas yield.

Acknowledgements

This work is in part supported by ISTC 2529 Project and Integration Project 39 and 110 of SB RAS.

References

[1] C. Song, Catal. Today 77 (2002) 17.
[2] M. Lyubovsky, L.L. Smith, M. Castaldi, H. Carim, B. Nentwick, S. Etemad, R. LaPierre, W.C. Pfefferle, Catal. Today 83 (2003) 71.
[3] D.A. Hickman, L.D. Schmidt, J. Catal. 138 (1992) 267.
[4] A. Cybulski, J.A. Moulijn, Catal. Rev. Sci. Eng. 36 (1994) 179.
[5] P. Aghalayam, Y.K. Park, D.G. Vlachos, Catalysis 15 (2000) 98.
[6] K.H. Hofstad, B. Andersson, A. Holmgren, O.A. Rokstad, A. Holmen, Stud. Surf. Sci. Catal. 119 (1998) 759.
[7] I. Tavazzi, A. Beretta, G. Groppi, P. Forzatti, Chem. Eng. Trans. 3 (2003) 213.
[8] M.-F. Reyniers, C.R.H. Smet, P.G. Menon, G.B. Marin, CATTECH 6 (2002) 140.
[9] R. Schwiedernoch, S. Tischer, C. Correa, O. Deutschmann, Chem. Eng. Sci. 58 (2003) 633.
[10] C.R.H. Smet, M.H.J.M. Groon, R.J. Berger, G.B. Marin, J.C. Schouten, Chem. Eng. Sci. 56 (2001) 4849.
[11] J. Lezaun, J.P. Gomez, M.D. Blanco, I. Cabrera, M.A. Pena, J.L.G. Fierro, Stud. Surf. Sci. Catal. 119 (1998) 729.
[12] S.N. Pavlova, N.N. Sazonova, Yu. A. Ivanova, V.A. Sadykov, O.I. Snegurenko, V.A. Rogov, Catal. Today 91–92 (2004) 299.
[13] V.A. Sadykov, G.M. Alikina, T.G. Kuznetsova, et al. Catal. Today 93–95 (2004) 45.
[14] G. Groppi, E. Tronconi, P. Forzatti, Catal. Rev. Sci. Eng. 41 (1999) 227.
[15] D. Dissanayke, M.P. Rosynek, K.C.C. Kharas, J.H. Lunsford, J. Catal. 132 (1991) 117.
[16] Z.-W. Liu, K.-W. Jun, H.-S. Roh, S.-C. Baek, S.-E. Park, J. Mol. Catal. A 189 (2002) 283.